Catalysis Communications 21 (2012) 52–57

Contents lists available at SciVerse ScienceDirect

Catalysis Communications

journal homepage: www.elsevier.com/locate/catcom

Short Communication

The effect of crystal sizes of HZSM-5 zeolites in ethanol conversion to propylene

Tao Meng, Dongsen Mao *, Qiangsheng Guo, Guanzhong Lu

Research Institute of Applied Catalysis, School of Chemical and Environmental Engineering, Shanghai Institute of Technology, Shanghai 201418, PR China

ARTICLE INFO

Article history:
Received 5 December 2011
Received in revised form 30 January 2012
Accepted 31 January 2012
Available online 10 February 2012

Keywords:
HZSM-5 zeolite
Crystal size
Ethanol to propylene

ABSTRACT

Three ZSM-5 zeolites with different crystal sizes were prepared and characterized by SEM, XRD, adsorption/desorption of N_2, NH_3-TPD, Py-IR and TG-DTA techniques. The results show that the acidic properties of HZSM-5 catalysts are very similar, but their textual properties are strongly influenced by crystal size. Their catalytic performances for the ethanol conversion to propylene were investigated in a continuous flow fixed-bed micro-reactor. In comparison with the large-sized HZSM-5, the small-sized HZSM-5 shows higher propylene selectivity and better stability, which reveals that decreasing the crystal size of zeolite is of benefit to ethanol conversion to propylene.

1. Introduction

Nowadays, propylene is mainly produced as a byproduct of naphtha steam cracking and catalytic cracking of crude oil. The petroleum crisis and the growing demand for propylene combined with environmental protection have driven many researchers to seek alternative resources to petroleum [1]. Currently, ethanol can be widely and easily produced by the fermentation from renewable biomass feed-stocks such as corn, sugarcane and cellulose [2]. Therefore, the development of processes for the production of propylene from ethanol has attracted more and more attention [3–8].

The effect of Si/Al ratio and metal modification of HZSM-5, as well as reaction conditions on the conversion of ethanol to propylene have been reported by some researchers [3–8]. For example, by modification with zirconium [5], strontium [6] or phosphorus [7] of HZSM-5, high propylene selectivity (about 30%) has been obtained, but it could not be sustained for a long time. For poor catalyst stability and resistance to coke formation of the zeolites, this process is insufficient for industrialization until now. Thus, further study is highly needed to enhance the catalytic performance of HZSM-5 in ethanol conversion to propylene.

Many researchers reported that the physico-chemical and catalytic properties of HZSM-5 zeolite were affected greatly by the crystal size [9–11]. However, to the best of our knowledge, there has been no report to clarify the influence of the crystal size of HZSM-5 catalyst on the ethanol to propylene process. In this work, three ZSM-5 zeolites with the same Si/Al molar ratio (~70) but different crystal sizes were synthesized, and the effect of crystal size on the activity and selectivity of the HZSM-5 catalyst toward the ethanol to propylene reaction was investigated for the first time.

2. Experiment

2.1. Catalyst preparation

All ZSM-5 samples were synthesized from a clear gel solution with a molar composition of 36 TPAOH:1 Al_2O_3:150 SiO_2:2300 H_2O. First, the required amount of aluminum isopropoxide and deionized water were added to the 50 wt.% aqueous solution of tetraproplammonium hydroxide (TPAOH). The mixture was stirred at 0 °C to obtain a clear solution. Second, tetraethylorthosilicate (TEOS) was added dropwise to the clear solution under stirring at room temperature. Then, the obtained solution was stirred at room temperature overnight to hydrolyze the TEOS completely.

The final solution obtained above was divided into three parts labeled as A, B and C, and three different strategies were used for synthesizing ZSM-5 with different crystal sizes. All of the three parts were crystallized in a Teflon-lined stainless-steel autoclave under autogenous pressure. Part A was crystallized under static conditions at 170 °C for 30 h. The crystallization reaction of part B was first carried out at 100 °C for 24 h and then rapidly changed into the second stage temperature of 170 °C for 30 h. Part C was primarily heated at 80 °C to remove alcohols and partial water, then the crystallization process of the concentrated solution obtained was as the same as that of part B.

After crystallization, the solid product was recovered after several cycles of centrifuging and washing with deionized water, dried overnight at 110 °C and calcined in air at 600 °C for 6 h. The obtained ZSM-5 was turned into the H-form by three consecutive ion exchanges in a large excess of aqueous 1 M solution of NH_4NO_3 at 90 °C and calcining again at 550 °C for 6 h. The HZSM-5 samples

* Corresponding author. Tel.: +86 21 60877221; fax: +86 21 60877231.
E-mail address: dsmao@sit.edu.cn (D. Mao).

1566-7367/$ – see front matter © 2012 Elsevier B.V. All rights reserved.
doi:10.1016/j.catcom.2012.01.030

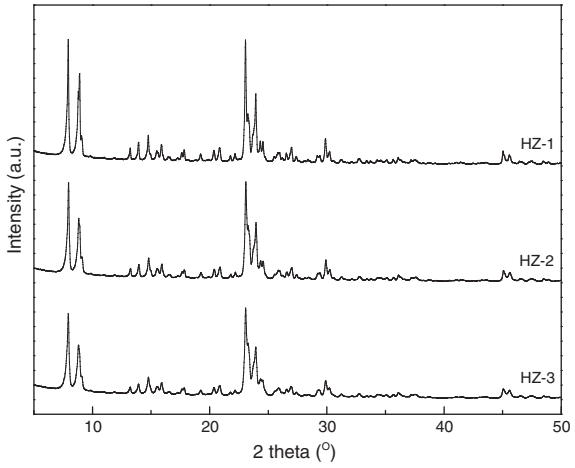

Fig. 1. XRD patterns of HZSM-5 zeolites with different crystal sizes.

prepared by part A, B and C were denoted as HZ-1, HZ-2 and HZ-3, respectively.

2.2. Catalyst characterization

XRD analysis of sample was performed using a PANalytical X'Pert diffractometer operating with Ni β-filtered Cu Kα radiation at 40 kV and 40 mA. SEM micrographs were obtained using a Hitachi S-4000 equipment. The bulk Si/Al molar ratios of the samples were determined by ICP-OES (PerkinElmer Optima 7000DV).

Nitrogen adsorption/desorption isotherms at −196 °C were obtained after outgassing the sample under vacuum at 200 °C for 12 h, using a Micromeritics ASAP2020 M+C adsorption apparatus.

NH_3-TPD was carried out on a conventional flow apparatus equipped with a TCD. The Py-IR spectra were recorded using a Nicolet 6700 infrared spectrometer with a resolution of 4 cm^{-1}. A self-supported 12 mm diameter circular wafer was placed in an infrared cell with CaF_2 windows and connected to a vacuum system. The wafer was dehydrated at 400 °C and at $P<10^{-2}$ mbar for 150 min. After cooling to room temperature, pyridine vapors were adsorbed for 30 min. Finally, excess pyridine was desorbed by evacuation of the sample at the desired temperature for 30 min, and IR spectra of adsorbed pyridine were recorded.

Coke amount was determined by a thermogravimetric analyzer (Shimadzu DTG-60H), with spent samples in air from 30 °C to 850 °C at a heating rate of 10 °C min^{-1}.

2.3. Catalyst test

Catalytic reaction tests were conducted at 500 °C under atmospheric pressure in a conventional continuous flow fixed-bed reactor made of stainless steel (inner diameter 6 mm). 0.3 g of catalyst was placed in the center zone of the reactor. Prior to the catalytic measurements, the fresh catalyst was activated at 500 °C for 1 h in nitrogen flow. Ethanol (purity > 99.5%) was pumped through a piston pump (WHSV of ethanol was 1.58 h^{-1}). Effluent products were analyzed online via an Agilent 6820 gas chromatograph equipped with a FID and a HP-Plot-Q capillary column. To avoid possible condensation of heavier hydrocarbons, the temperature of the effluent line was constantly maintained at 180 °C.

3. Results and discussion

3.1. Characterization of catalysts

XRD patterns of the synthesized products exhibit the typical XRD patterns corresponding to the pure MFI structure (Fig. 1). The very low background signal and sharp reflections indicate excellent crystallinity of the samples. The decrease in peak intensity and

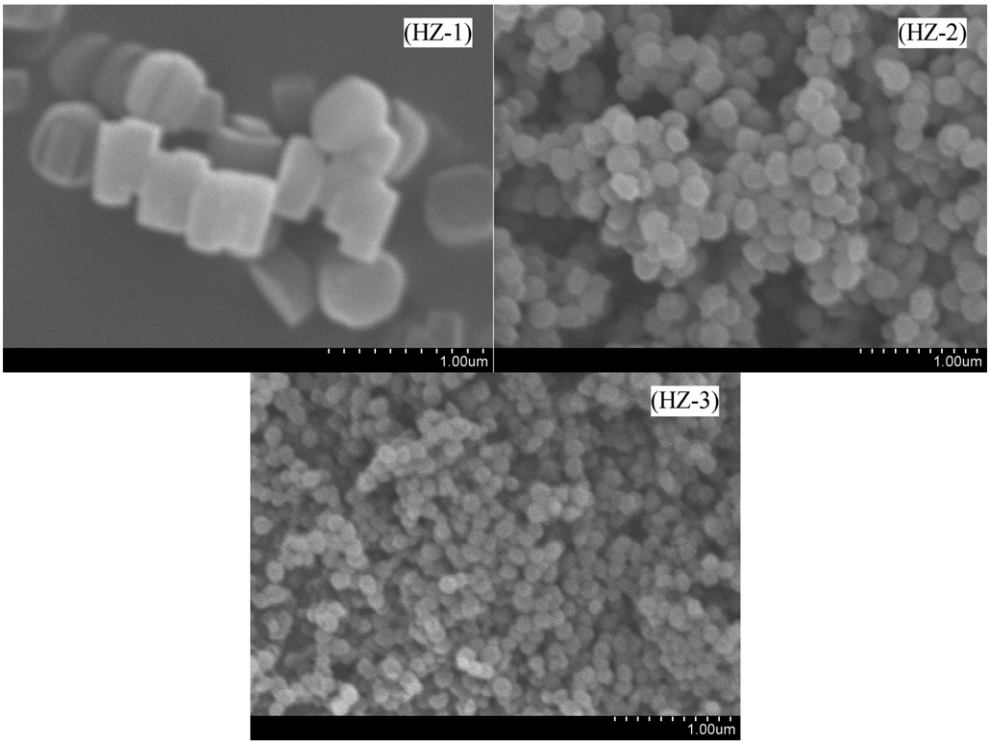

Fig. 2. SEM images of HZSM-5 zeolites with different crystal sizes.

Table 1
Specific surface area, pore volume, pore diameter and Si/Al molar ratios of HZSM-5 zeolites with different crystal sizes.

Sample	Surface area ($m^2\ g^{-1}$)			Pore volume($cm^3\ g^{-1}$)			Average pore diameter (nm)	Si/Al molar ratio[a]
	Total	Micropore	External	Total	Micropore	Mesopore		
HZ-1	347	133	214	0.23	0.04	0.19	2.65	73
HZ-2	372	146	226	0.40	0.05	0.35	4.30	70
HZ-3	387	154	233	0.53	0.07	0.46	5.48	70

[a] Determined by ICP-OES.

increase in line width from HZ-1 to HZ-3 can be attributed to the decrease in crystal size of the sample [12].

As shown in Fig. 2, the average particle sizes of HZ-1, HZ-2 and HZ-3 are about 500 nm, 250 nm and 100 nm, respectively. The decrease in crystal size from HZ-1 to HZ-3 is in good agreement with the XRD result. It indicates that the crystal size of ZSM-5 zeolite can be adjusted effectively by varying the crystallization temperature [13] and the concentration of the mother-gel [14] in the synthesis process. The Si/Al molar ratios of the prepared HZSM-5 samples, as measured by ICP-OES, are fairly similar regardless of the crystal size (Table 1).

From Table 1, it can be seen that both the micropore surface area and external surface area increase with decreasing crystal sizes, which can be attributed to the structural differences among the three samples [15]. The volumes of mesopores and average pore diameter also increase with decreasing crystal sizes, which is probably owing to the different aggregation extent of the samples [16]. As shown in Fig. 2, the aggregation extent of HZSM-5 particles increased with decreasing the crystal sizes, resulting in the larger average pore diameter due to more secondary pores formed by aggregation. On the contrary, the micropore volumes are fairly close for all the HZSM-5 samples (Table 1).

As shown in Fig. 3, the N_2 adsorption/desorption isotherms for all the HZSM-5 samples exhibit a hysteresis loop, which usually associates with the filling and emptying of mesopores originating from the inter-particle space of crystalline agglomerates by capillary condensation. Furthermore, the hysteresis loop becomes larger from HZ-1 to HZ-3, indicating that the smaller-sized HZSM-5 sample has larger pores [10].

As shown in Fig. 4, all the HZSM-5 catalysts show a typical NH_3-TPD spectrum with two maximum peaks below and above 300 °C, corresponding to NH_3 eluted from the weak and strong acid sites, respectively. It can be seen clearly that though crystal sizes are different for the three HZSM-5 samples, there is only a marginal difference in the acidic properties (both the strength and amount of the acidic sites) among them. This observation is in good line with our previous result [17].

The spectra of pyridine on the HZSM-5 samples exhibit the characteristic bands at 1544 and 1446 cm^{-1}, which are attributed to pyridinium ions (pyridine chemisorbed on Brönsted acidic sites)

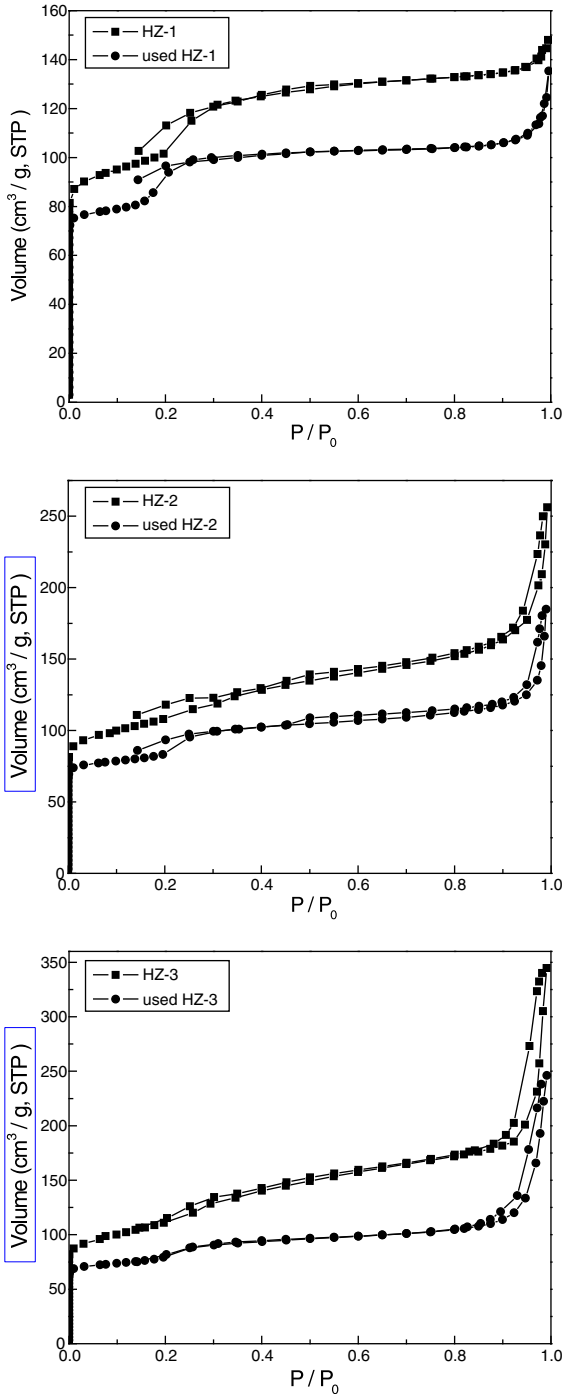

Fig. 3. N_2 adsorption/desorption isotherms of the fresh and used HZSM-5 samples.

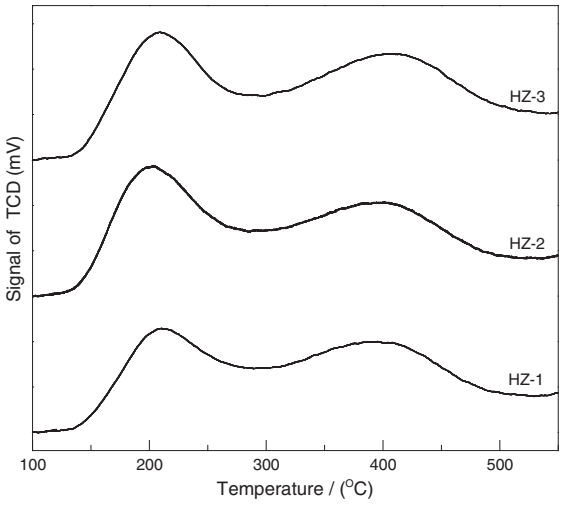

Fig. 4. NH_3-TPD curves of HZSM-5 zeolites with different crystal sizes.

Table 2
Result of IR spectra of Py adsorbed on the different HZSM-5 zeolites after desorption at different temperatures.

Sample	100 °C			300 °C		
	A_B	A_L	Total	A_B	A_L	Total
HZ-1	0.36	0.46	0.82	0.27	0.10	0.37
HZ-2	0.42	0.47	0.89	0.29	0.09	0.38
HZ-3	0.41	0.61	1.02	0.32	0.10	0.42

and coordinatively bound pyridine (pyridine interacting with Lewis acidic sites), respectively. The intensities of the bands at 1544 and 1446 cm^{-1} were used to calculate the concentrations of acidic sites of HZSM-5 samples [18]. The data (Table 2) show that HZSM-5 zeolites with different crystal sizes have similar concentration of both Brönsted and Lewis acidic sites at the same desorption temperature (especially at higher temperature), considering the relatively big experimental error of the method. This result is in agreement with that of NH_3-TPD technique. In conclusion, ZSM-5 zeolites with the same Si/Al ratio and acidity could be obtained irrespective of their crystal sizes.

3.2. Catalytic performance

The catalytic activity and selectivity for the conversion of ethanol into propylene had been investigated over the as-prepared HZSM-5 catalysts, which had similar physico-chemical properties except for the crystal size. For all the samples, the conversion of ethanol was 100% during the whole operation; however, the product selectivity was remarkably different.

The effects of time on stream on the selectivity to light (C_2–C_4) olefins and aromatics for each sample are shown in Fig. 5. For the HZ-1 with the biggest crystal size, the propylene selectivity is the lowest, and the propylene selectivity falls below 11% after 28 h on steam. The propylene selectivity of HZ-2 is slightly higher than that of HZ-1, and the stability of the catalyst is also improved. The advantages are even more pronounced for HZ-3: the propylene selectivity increases further and the stability is even better than that on HZ-2. Thus, it is concluded that the increased propylene selectivity and stability can be attributed to decrease of the crystal size. As the small crystal has shorter channels, the reactants contact with fewer number of acidic sites and diffuse quickly, which suppresses effectively the secondary reaction of propylene [15,19]. The selectivity to $C_4^=$ of the catalysts decreases from HZ-3 to HZ-1, which is same to propylene selectivity.

As presented in Fig. 5, the ethylene selectivity of all HZSM-5 catalysts increased with time; however, the selectivity for aromatics decreased with time. As described by Inoue et al. [20], lower surface acidity led to the formation of more ethylene, while aromatics were promoted at higher acidity. During the ethanol conversion reaction, coke formed and covered the strong acidic sites of the catalyst. Thus, ethanol dehydration to ethylene reaction can still occur on

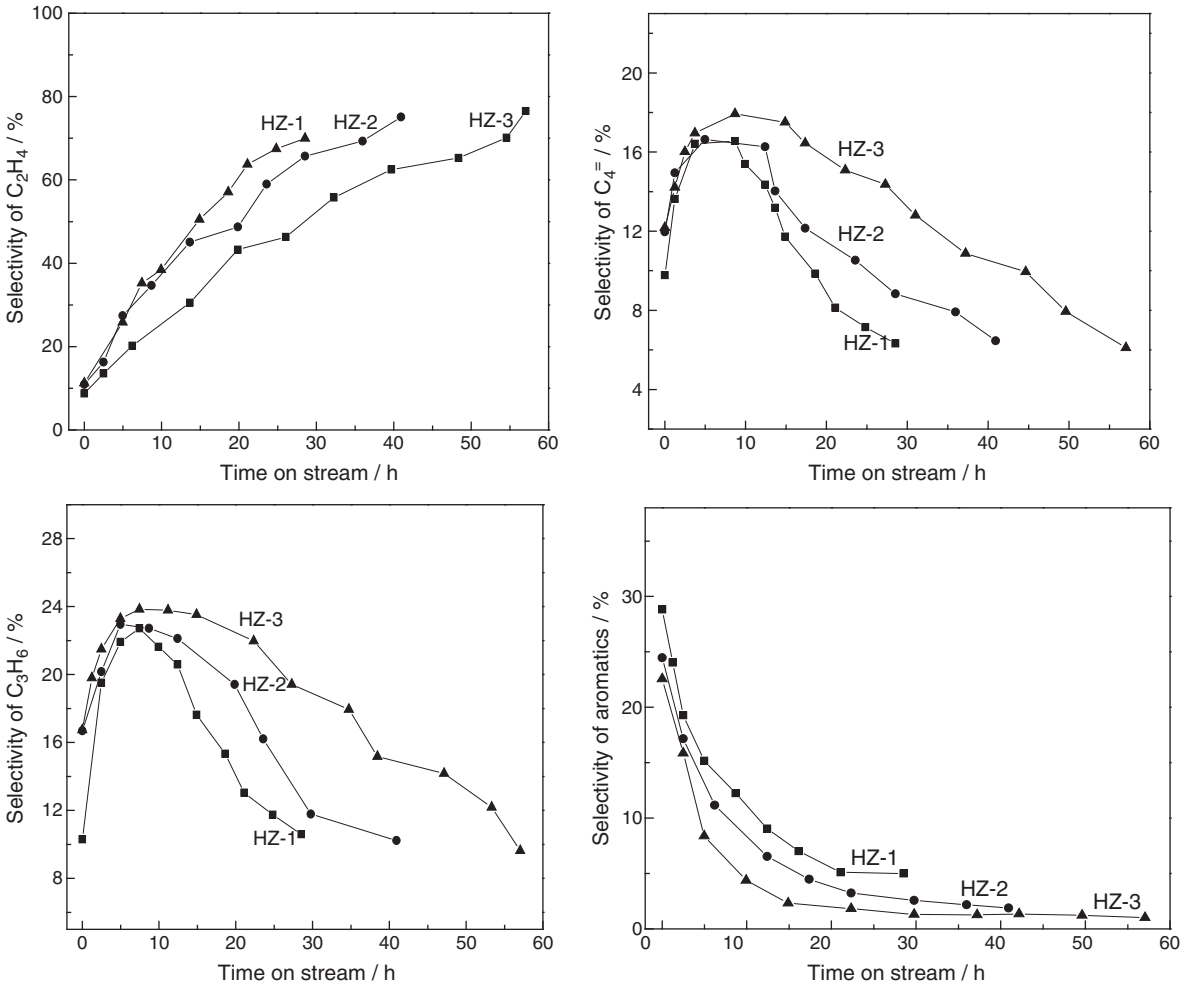

Fig. 5. Effect of time on stream on selectivity of C_2–C_4 olefins and aromatics over HZSM-5 zeolites with different crystal sizes.Reaction conditions: atmospheric pressure; $T = 500$ °C; WHSV = 1.58 h^{-1}.

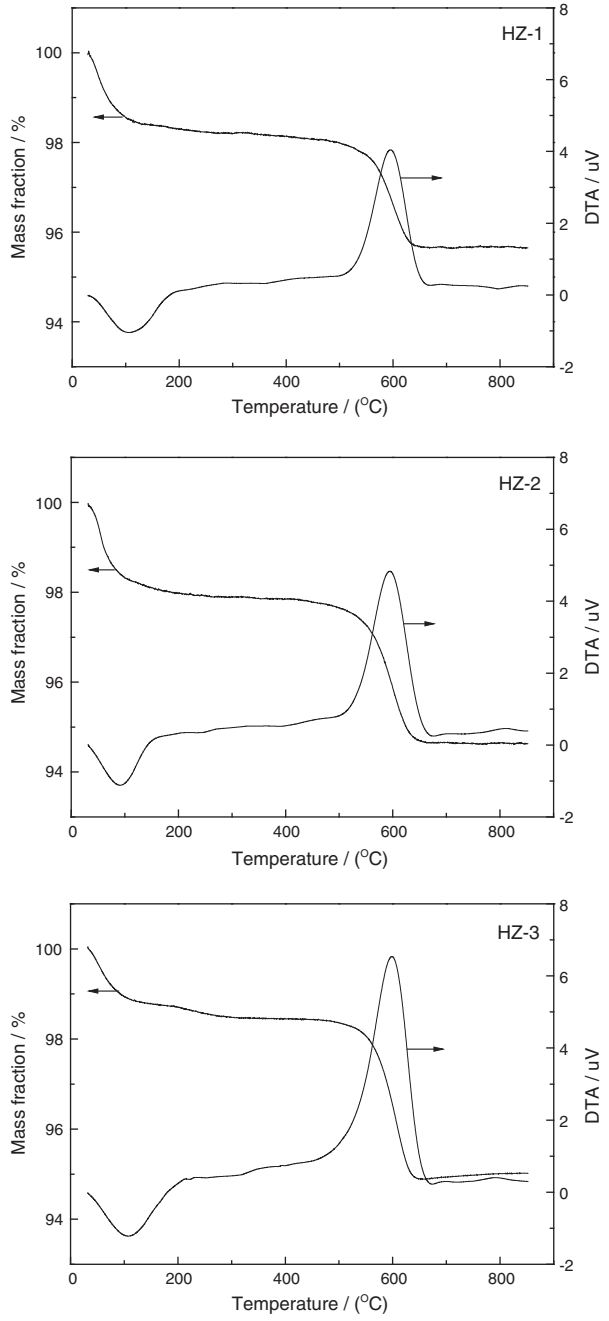

Fig. 6. TG-DTA curves of HZSM-5 zeolites with different crystal sizes after the duration test of ethanol to propylene catalytic reaction.

weak acidic sites, whereas the subsequent reaction steps cannot happen for they require sites of higher acidic strength [21]. In summary, the selectivity variation trend of ethylene and aromatics can be explained by the deactivation of the strong acidic sites [15].

Coke deposition might be the main reason for the decreasing of propylene selectivity, since the samples were black in color after the reaction [22]. As shown in Fig. 6, the appearance of an abrupt and large weight loss in 400–700 °C with a broad exothermic peak around 600 °C clearly indicates the vigorous combustion of coke of all the used HZSM-5 catalysts. Besides, the endothermic peak at around 100 °C corresponds to the evaporation of water of the used catalysts. The relative amounts of carbonaceous deposits for the used HZ-1, HZ-2 and HZ-3 samples are 2.5%/28.5 h, 3.2%/40.9 h and 3.5%/57.0 h, respectively. The result indicates that the ability to tolerate the coke deposit decreases in the order HZ-3 > HZ-2 > HZ-1 [12]. As the coke formation mainly occurs in the secondary pores [23], it can also be evidenced clearly from Fig. 3 that the hysteresis loops of the used HZ-2 and HZ-3 samples were smaller than those of the fresh HZ-2 and HZ-3 samples, respectively; the small-sized catalyst HZ-3 has more secondary pores (Table 1) to accommodate the coke deposits, so the stability of HZ-3 was enhanced. On the other hand, the average rate of coke formation on HZ-1/28.5 h, HZ-2/40.9 h and HZ-3/57.0 h are 9.00×10^{-4} g g_{cat}^{-1} h, 8.08×10^{-4} g g_{cat}^{-1} h and 6.36×10^{-4} g g_{cat}^{-1} h, respectively. The result clearly shows that the formation rate of coke increases along with the crystallite sizes. For the large-sized catalyst with long channels, the diffusion of the products is resisted, so secondary reaction of parts of the trapped primary products takes place to produce bulky aromatic molecules, which are the precursor of coke [24]. As described above, for the high formation rate of coke and the high diffusion resistance, the propylene selectivity of HZ-1 decreased rapidly with time. In contrast, for the small-sized catalyst with shorter channels and more pore mouths, the products would easily diffuse out of the pores, which suppresses the secondary reaction to form the precursor of coke and hence delays the blocking of the channel by coke [12,24].

4. Conclusions

The ZSM-5 zeolites with different crystal sizes but the same Si/Al ratio were successfully synthesized by varying the crystallization temperature and the concentration of the mother-gel in the synthesis process. With the crystallite size decreasing, the surface area, pore volume and pore diameter of the HZSM-5 zeolite increase. The small-sized sample shows higher propylene selectivity and better stability than larger-sized sample during the ethanol conversion testing due to its larger pore volume, more secondary pores, shorter channels, and reduced diffusion path lengths, which shows low formation rate of coke, low diffusion resistance and high ability to tolerate the coke.

Acknowledgements

The authors thank Shanghai Municipal Education Commission (J51503) and Graduate Innovation Foundation of Shanghai Institute of Technology (yjscx2010005) for financial support.

References

[1] J. Liu, C.X. Zhang, Z.H. Shen, W.M. Hua, Y. Tang, W. Shen, Y.H. Yue, H.L. Xu, Catalysis Communications 10 (2009) 1506.
[2] K. Ramesh, C. Jie, Y.F. Han, A. Borgna, Industrial and Engineering Chemistry Research 49 (2010) 4080.
[3] W. Xia, A. Takahashi, I. Nakamura, H. Shimada, T. Fujitani, Journal of Molecular Catalysis A: Chemical 328 (2010) 114.
[4] K. Inoue, M. Inaba, I. Takahara, K. Murata, Catalysis Letters 136 (2010) 14.
[5] Z.X. Song, A. Takahashi, N. Mimura, T. Fujitani, Catalysis Letters 131 (2009) 364.
[6] D. Goto, Y. Harada, Y. Furumoto, A. Takahashi, T. Fujitani, Y. Oumi, M. Sadakane, T. Sano, Applied Catalysis A: General 383 (2010) 89.
[7] Z.X. Song, A. Takahashi, I. Nakamura, T. Fujitani, Applied Catalysis A: General 384 (2010) 201.
[8] K. Inoue, K. Okabe, M. Inaba, I. Takahara, K. Murata, Reaction Kinetics, Mechanisms and Catalysis 101 (2010) 477.
[9] M. Singh, R. Kamble, N. Viswanadham, Catalysis Letters 120 (2008) 288.
[10] K.Y. Wang, X.S. Wang, Microporous and Mesoporous Materials 112 (2008) 187.
[11] Y. Wang, L.F. Guo, Y. Ling, Y.M. Liu, X.H. Li, H.H. Wu, P. Wu, Applied Catalysis A: General 379 (2010) 45.
[12] X.J. Cheng, X.S. Wang, H.Y. Long, Microporous and Mesoporous Materials 119 (2009) 171.
[13] Q. Li, D. Creaser, J. Sterte, Microporous and Mesoporous Materials 31 (1999) 141.
[14] R.V. Grieken, J.L. Sotelo, J.M. Menéndez, J.A. Melero, Microporous and Mesoporous Materials 39 (2000) 135.
[15] M. Firoozi, M. Baghalha, M. Asadi, Catalysis Communications 10 (2009) 1582.
[16] P.Q. Zhang, X.W. Guo, H.C. Guo, X.S. Wang, Journal of Molecular Catalysis A: Chemical 261 (2007) 139.
[17] D.S. Mao, Q.S. Guo, G.Z. Lu, Acta Petrolei Sinica (Petroleum Processing Section) 25 (2009) 503.
[18] D.S. Mao, W.M. Yang, J.C. Xia, B. Zhang, Q.Y. Song, Q.L. Chen, Journal of Catalysis 230 (2005) 140.

[19] D. Chen, K. Moljord, T. Fuglerud, A. Holmen, Microporous and Mesoporous Materials 29 (1999) 191.
[20] K. Inoue, K. Okabe, M. Inaba, I. Takahara, K. Murata, Reaction Kinetics, Mechanisms and Catalysis 101 (2010) 227.
[21] A.T. Aguayo, A.G. Gayubo, A.M. Tarrío, A. Atutxa, J. Bilbao, Journal of Chemical Technology and Biotechnology 77 (2002) 211.
[22] N.R.C.F. Machado, V. Calsavara, N.G.C. Astrath, A.M. Neto, M.L. Baesso, Applied Catalysis A: General 311 (2006) 193.
[23] P.Q. Zhang, X.S. Wang, X.W. Guo, H.C. Guo, L.P. Zhao, Y.K. Hu, Catalysis Letters 92 (2004) 63.
[24] H. Mochizuki, T. Yokoi, H. Imai, R. Watanabe, S. Namba, J.N. Kondo, T. Tatsumi, Microporous and Mesoporous Materials 145 (2011) 165.